2023 IEEE International Conference on Robotics and Automation (ICRA 2023)
May 29 - June 2, 2023. London, UK

# STEV: Stretchable Triboelectric E-skin enabled Proprioceptive Vibration Sensing for Soft Robot

Zihan Wang*, Kai-Chong Lei*, Huaze Tang, Shoujie Li, Yuan Dai,
Wenbo Ding, and Xiao-Ping Zhang, *Fellow, IEEE*

***Abstract*— Vibration perception is essential for robotic sensing and dynamic control. Nevertheless, due to the rigorous demand for sensor conformability and stretchability, enabling soft robots with proprioceptive vibration sensing remains challenging. This paper proposes a novel liquid metal-based stretchable e-skin via a kirigami-inspired design to enable soft robot proprioceptive vibration sensing. The e-skin is fabricated into 0.1mm ultrathin thickness, ensuring its negligible influence on the overall stiffness of the soft robot. Moreover, the working mechanism of the e-skin is based on the ubiquitous triboelectrification effect, which transduces mechanical stimuli without external power supply. To demonstrate the practicability of the e-skin, we built a soft gripper consisting of three soft robotic fingers with proprioceptive vibration sensing. Our experiment shows that the gripper can accurately distinguish the grain category (six grains with the same mass, 99.9% accuracy) and the packaging quality (100% accuracy) by simply shaking the gripped bottle. In summary, a soft robotic proprioceptive vibration sensing solution is proposed; it helps soft robots to have a more comprehensive awareness of their self-state and may inspire further research on soft robotics.**

## I. Introduction

Motivated by the multimodal sensing capability of biological skin, electronic skin (e-skin) was developed to be mounted on or embedded into healthcare devices, prosthetics, and robotics to enable multifarious sensory functions [1]. Stretchable e-skin with exceptional flexibility and conformability allows seamless coverage of complex soft robot surfaces while reducing the hindrance to the mobility of soft actuators [2]. However, developing an e-skin to precept soft robots' self-vibration status is challenged by compatible design and fabrication to constitute the sensing elements and soft bodies as a whole [3]. In fact, vibration information is essential for robotics study. From detecting the slippage of delicate objects [4] to actively canceling the undesired damping upon actuation [5], vibration sensing takes an irreplaceable position. However, existing vibration sensors (*e.g.* inertial measurement unit, IMU) are made of rigid materials, which are mechanically mismatched with soft robots. Therefore, seamlessly fusing vibration sensory into soft robots without sacrificing flexibility and dexterity remains an open problem [6].

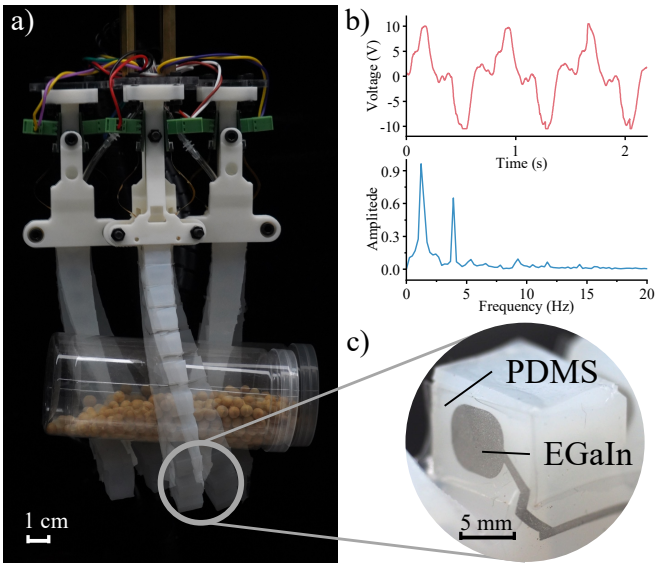


Fig. 1. System overview. (a) A soft gripper with proprioceptive vibration sensing is shaking a bottle of soybeans. (b) The voltage output of the triboelectric e-skin in time and frequency domains. (c) Enlarged photograph of the triboelectric e-skin.

To tackle this challenge, we propose a stretchable e-skin to enable soft robot proprioceptive vibration sensing. The e-skin is fabricated by screen print metal-polymer conductors (MPCs), which is highly conductive, low cost, and mass-manufacturable [7]. By utilizing the ubiquitous contact electrification and electrostatic induction effect [8], we tactfully leverage the triboelectric charge density difference between the material of the soft robot body (silicon elastomer) and e-skin substrate (polydimethylsiloxane, PDMS) [9] to realize self-powered vibration sensing of the soft body. According to the best knowledge of the authors, there has been no similar design for soft robot's proprioceptive vibration sensing before. To demonstrate the practicability of the e-skin, we built STEV, a soft gripper composed of three PneuNet-type [10] fingers with the e-skin installed. As Fig. 1 shows, the gripper can distinguish the grains category by shaking the container and analyzing the frequency profile from the e-skin's output. The classification result revealed that even a basic machine

* The first two authors contributed equally to this work.

This work is supported in part by the National Natural Science Foundation of China 62104125, by Tencent Robotics X Lab, by the Guangdong Basic and Applied Basic Research Foundation 2020A1515110887, and by Shenzhen Science and Technology Program JCYJ20220530143013030.

Z. Wang, K.-C. Lei, H. Tang, S. Li, W. Ding, and X.-P. Zhang are with Tsinghua-Berkeley Shenzhen Institute, Shenzhen International Graduate School, Tsinghua University, China. W. Ding is the corresponding author. E-mail:{zhwang22, liqc21, thz21, lsj20} @mails.tsinghua.edu.cn, {ding.wenbo, xiaoping.zhang} @sz.tsinghua.edu.cn

Y. Dai is with Tencent Robotics X Lab, Shenzhen, China. E-mail: jessiedai@tencent.com.

W. Ding and X.-P. Zhang are also with RISC-V International Open Source Laboratory, Shenzhen, China, 518055.

X.-P. Zhang is also with the Department of Electrical, Computer and Biomedical Engineering, Ryerson University, Toronto, ON M5B 2K3, Canada.

2023 IEEE International Conference on Robotics and Automation (ICRA) | 979-8-3503-2365-8/23/$31.00 ©2023 IEEE | DOI: 10.1109/ICRA48891.2023.10160790

learning (ML) model can receive 99% accuracy in classifying six kinds of grains. STEV is also capable of facilitating industrial applications by its vibration response, such as packaging quality inspection. In our test, four protective foam filling conditions can be 100% accurately detected. The contributions of this work can be summarized in threefold:

- A novel stretchable e-skin design is proposed to enable soft robots with proprioceptive vibration sensory.
- A low-cost, scalable and massive producible e-skin fabrication process is proposed, which can easily be generalized to a broad spectrum of soft robots.
- We design experiments to demonstrate soft robot proprioceptive vibration sensing applied in service and industrial tasks, such as food ingredients identification and packaging quality inspection.

## II. Related Works

Standing at the crossroad of material science and information technology, e-skin enables soft robots to sense external stimuli and perceive their physical status [6]. One important purpose of applying e-skins on soft robots is to sense the surrounding environment and facilitate output optimal action parameters. Towards this purpose, e-skin often appears in different forms of tactile sensors. From resistive-based 3D object models reconstruction [11] to capacitive array enabled fragile objects manipulation [4], from magnetic super-resolution skin [12] to triboelectric material identification fingertip [13], [14], the tactile sensor has come a long way. Meanwhile, another major purpose of installing e-skin on soft robots is to sense the robot's self-state, also known as proprioceptive sensing [15]. Although advanced sensing techniques such as fiber Bragg gratings [16] and stretchable optical waveguides [17], [18] can enable soft robots proprioception. Yet, these solutions more or less sacrifice the overall compliance of soft robots. Thus, in soft robotics, there is a dilemma between proprioception and compliance. Besides, the current exploration of soft robots' proprioception mainly focuses on reconstructing soft robots' 3D configurations [19] and 2D bending angles [20]. Perception of other self-state properties of soft robots, such as vibration, is often neglected.

In practice, the vibration status of robots can provide much valuable information, such as identifying the texture of objects by slippage vibration [21], predicting the liquid properties by post-shaking oscillation [22], and identifying solid items in different containers by contact [23]. Among various vibration transducers, the triboelectric-based ones have high energy efficiency [24] and ultra-wide bandwidth [25]. The emerging triboelectric nanogenerator (TENG) invented by Wang *et al.* in 2012 [26] provides a wide range of material selection for self-powered sensors [27] and energy harvesters [28]. And TENG combined flexible sensors, as well as soft actuators, are also actively contributing to the development of robotics, especially for the soft robotics community [29], [30].

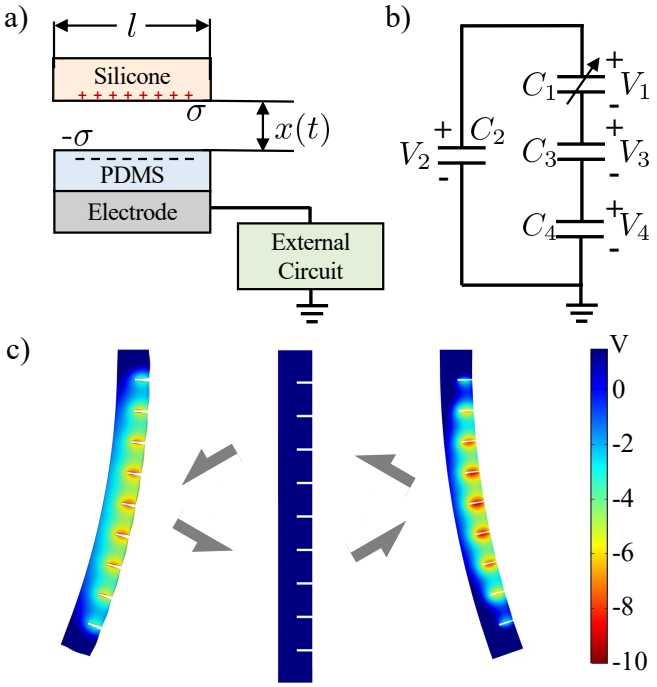


Fig. 2. (a) Structural schematic diagram of single electrode triboelectric sensor. (b) Equivalent circuit model of single electrode triboelectric sensor. (c) COMSOL simulation of electric field distribution in different bending states of a PneuNet soft finger.

## III. Design and Fabrication

Soft robots feature their embodied compliance. To minimize the adverse effect on the softness of the robots, Young's modulus of e-skins mounted on their surfaces should be as low as possible. Therefore, we select a metal-polymer conductor-based elastic circuit fabrication technique [7] to create the e-skin. The vibration sensing mechanism of the stretchable e-skin is also elaborated on in this section.

### A. Triboelectric sensing mechanism

Triboelectrification, also called contact electrification, is a ubiquitous phenomenon between contact interfaces in various materials. The structure of the triboelectric sensor node can be modeled as Fig. 2(a) shows, where each sensor node consists of a eutectic gallium-indium (EGaIn) electrode layer and two dielectric layers made by silicone and PDMS, respectively. Both electrode layer and dielectric layers have the same length $l$ and width $w$. The gap between the dielectric layer is denoted as $x(t)$. After contact occurs, the silicone surface accumulates positive charges with density $\sigma$, while the PDMS surface induces an equal amount of negative charges. The mechanism of the sensor can be explained in terms of Maxwell's displacement current. With the presence of electric field $\mathbf{E}$ induced by charges on the surface of two dielectric layers, a polarized electric field $\mathbf{P}$ is generated between two layers. From Gauss's law of Maxwell's equations, Maxwell's displacement current density $\mathbf{J}_D$ can be expressed as follow in Eq. (1),

$$\mathbf{J}_D = \varepsilon_0 \frac{\partial \mathbf{E}}{\partial t} + \frac{\partial \mathbf{P}}{\partial t}, \tag{1}$$

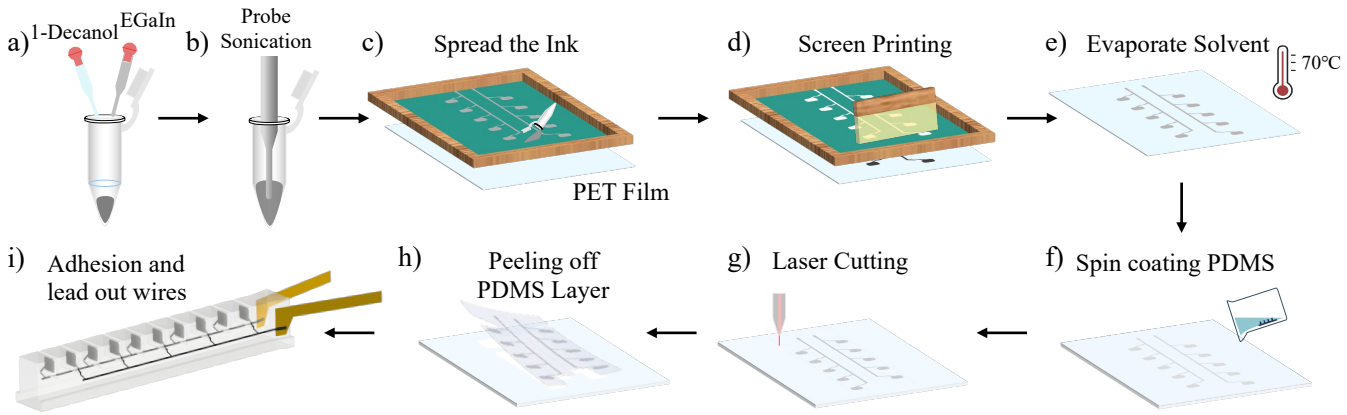


Fig. 3. Fabrication process of the e-skin. (a) Add materials to a centrifuge tube to prepare the MPC ink. (b) Disperse EGaIn by probe sonication. (c) Spread the MPC ink on the printing screen. (d) Screen printing the circuit. (e) Heating the PET substrate to evaporate the solvent of the ink. (f) Spin coating PDMS (600 rpm, 20 s) onto the PET substrate to envelope the EGaIn micro particle trace. (g) Laser cutting the sensing part according to the configuration of the soft finger. (h) Peeling of the PDMS layer which encapsulates the EGaIn micro particle trace. (i) Adhere the e-skin to the soft finger and connect flexible printed circuit connectors.

where $\varepsilon_0$ is the permittivity in vacuum. The first term $\varepsilon_0 \partial \mathbf{E}/\partial t$ excites electromagnetic wave that dissipates in space, and the second term $\partial \mathbf{P}/\partial t$ is directly related to the output voltage of the sensor [28], where we adopt the equivalent capacitance circuit model of TENG (Fig. 2(b)) to elaborate [8]. Herein, $C_1$ denotes the capacitance formed by two dielectric layers, $C_2$ is the capacitance between the silicone layer and ground, $C_3$ represents the internal capacitance of the PDMS layer, and $C_4$ refers to the self-capacitance of the electrode layer. According to the law of charge conservation, we can express $V_4$, the voltage between EGaIn electrode and ground at open circuit (OC) condition in Eq. (2),

$$V_{OC} = -\frac{\sigma w l C_2 C_3}{C_1 C_2 C_4 + C_1 C_3 C_4 + C_2 C_3 C_4}. \tag{2}$$

When the soft finger vibrates, the gap between chambers is squeezed and expanded, resulting in capacitance $C_1$ changes. Here, $C_1$ is modeled as a parallel plate capacitor so that we can write the relationship between $C_1$ and the gap width $x(t)$ as Eq. (3),

$$C_1 = \frac{\varepsilon_0 w l}{x(t)}, \tag{3}$$

where $\varepsilon_0$ represents the permittivity in the air and $x(t)$ is the distance between dielectric layers. Combining Eq. 2 and Eq. 3, the relationship between the output voltage and the gap distance between dielectric layers can be established.

Based on the above theoretical analysis, we simulate the electric field distribution of a soft robotic finger of STEV in different bending states by COMSOL multiphysics. According to the datasheet [31], the charge density of PDMS and silicon elastomer is set to -0.54 $\mu$C/m$^2$ and 0.54 $\mu$C/m$^2$, respectively. The dynamics model of the soft finger is also considered in the simulation. The Ogden hyperelastic model for soft materials is applied to simulate large-scale deformation in bending [32]. Fig. 2(c) shows the potential difference on both sides of the wall. Record the change of potential

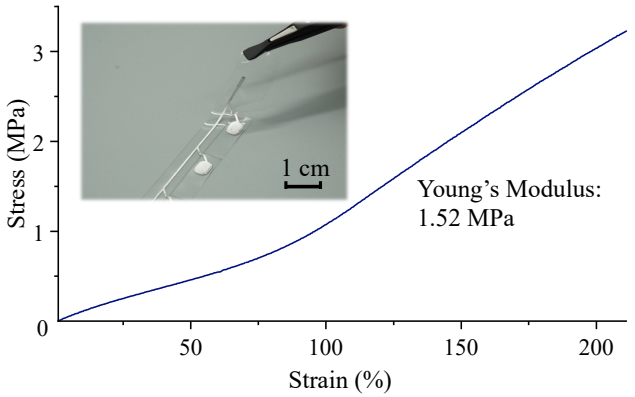


Fig. 4. Tensile testing curve of the stretchable e-skin.

difference will achieve the vibration's proprioception. Based on this concept, we fabricate a kirigami structured stretchable e-skin to deploy on a pneumatic-driven soft robot.

### *B. Fabrication of the e-skin*

The conductive substance of the elastic circuit, eutectic gallium-indium (EGaIn), is a type of non-toxic liquid alloy widely used in biomedical and wearable applications. Since EGaIn has extremely high surface tension (0.63 N/m [33]) and weak affinity to polymer or silicone, it is nearly impossible to direct pattern a long-standing circuit on a silicon soft body. Before patterning the circuit, MPC ink is prepared to reduce surface tension and boosted the polymer affinity of EGaIn. As Fig. 3(a-b) indicates, 3 g EGaIn and 0.5 ml 1-decanol are added into a centrifuge tube, and then the mixture is dispersed by an ultrasonic probe (JY92-IIN) for three minutes in ice-water bath. The sonication process can break the EGaIn chunk into 2 $\mu$m diameter microparticles [7]. The microparticles' small diameter enables MPC ink to readily pass through the printing screen mesh used in the following step, while the 1-decanol solvent increases the ink's affinity to the PET substrate film.

Screen printing is an efficient patterning technique adopted in industry, it can massively reproduce patterns with fine details. Here, we adopt the screen printing technique shown in Fig. 3(c-e) to pattern the elastic circuit. First, PDMS releasing agent is sprayed on a clean PET (polyethylene terephthalate) film to ensure the stretchable circuit can be easily detached from the PET substrate in the following steps. Before printing, we use a rubber scraper to evenly spread the liquid metal ink onto the screen mesh and place PET substrate film underneath the printing screen. Then, we pull the scraper to print the circuit on the PET substrate. Finally, the printed PET substrate will be placed in a 70 °C oven for 10 minutes to evaporate 1-decanol. Note that the circuit's color changes during the thermal processing, from the MPC ink's grey appearance to EGaIn micro particles' silver metallic luster.

After the patterning, the circuit is transferred from non-stretchable PET film to stretchable PDMS film by spin coating. Two pars of PDMS precursor are mixed by defoaming mixer (THINKY ARE310) for 45 s. Then, use a spin coater to evenly spread the mixed PDMS precursor on the PET film with the dry circuit. By adjusting the spinning speed to 600 rpm and spinning time to 20 s, the fabricated e-skin reaches 0.1 mm ultra-thin thickness. Cured PDMS is cut into a branch-and-leaves shape by a laser cutter and peeled from the substrate, as the inlet photograph in Fig.4 shows. The Young's modulus of the as-fabricated ultrathin stretchable e-skin reached 1.52 MPa (Fig.4), which is negligible to the soft robot's overall compliance. Finally, we lead out wires and adhere the e-skin to a PneuNet soft robotic finger to finish the assembly. The fabrication cost of each e-skin with lab materials only needs 0.5 US dollars. In massive manufacturing, the already fairly small cost will continue to decrease due to scale merit.

## IV. Experiment

To evaluate the vibration sensing capability of STEV, we have systematically devised three experiments: (1) Compare vibration sensing results from the e-skin and the commercial IMU. (2) Identify a bottle of grains with the same mass by oscillation. (3) Evaluate the packaging quality by oscillation.

### A. Vibration sensing performance comparison

Referring to the method proposed by Li *et al.* [5], we attached an IMU module (MPU 9250) at the bottom of a soft finger installed the e-skin as a reference for vibration sensing. The experiment test bench is depicted in Fig. 5a, where the triboelectric voltage output of the e-skin is recorded by NI 9220 with 1 GΩ resistor connected in parallel for input impedance matching. The oscillation of STEV is realized by a linear motor (LinMot, H01-37x166/280) that performs 1 Hz reciprocating motion (40mm displacement, 1 m/s$^2$ acceleration, and 0.5 m/s maximum speed). It can be seen from Fig. 5b-c that the 1 Hz base resonance mode mostly dominates the triboelectric signal. The smaller high-order harmonics in triboelectric signal is due to the intrinsic capacitance of the triboelectric sensor and the external input

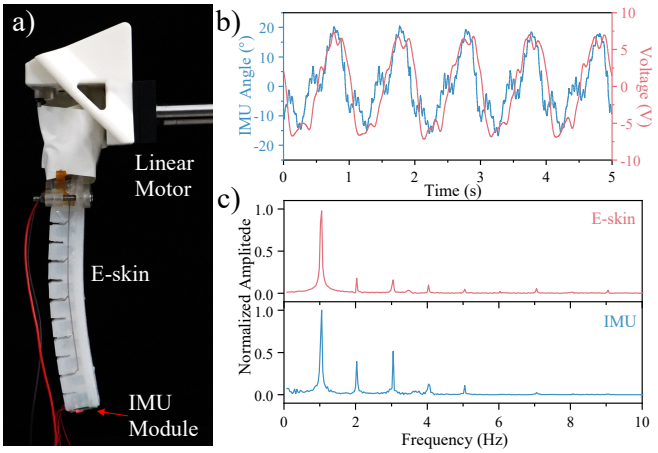


Fig. 5. (a) System set-up for the sensor's reading comparison with IMU. (b) Time domain comparison. (c) Frequency domain comparison.

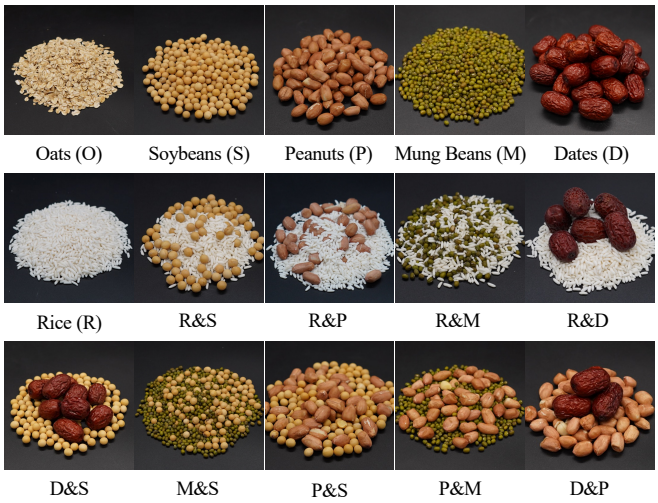


Fig. 6. Six single-ingredient grains and nine dual-ingredients grains.

matching resistor forms a natural low-pass filter, which is highly beneficial for practical applications [34].

### B. Grain identification

To illustrate that STEV can capture subtle vibration differences, we designed an experiment that classifies a bottle of different grains (Fig. 6) with the same mass by simply shaking them. The air pressure that drives STEV to ensure securely holding the bottle is maintained at 50 kPa during actuation by Cordis closed-loop pressure control valve. And the shaking is achieved by the same linear motor with 1.3 Hz reciprocating motion (80 mm displacement, 4 m/s$^2$ acceleration, and 1 m/s maximum speed).

In each signal acquisition cycle, the soft gripper shakes a bottle filled with 100 g grains for 10 times in 15 s. The dataset of each object class contains 10 acquisitions. For each class, we split the data from six channels into 600 samples and perform principal component analysis (PCA) to extract the principal oscillation component. To further enhance data efficiency, Fourier transformation is conducted, and the obtained frequency domain components are truncated

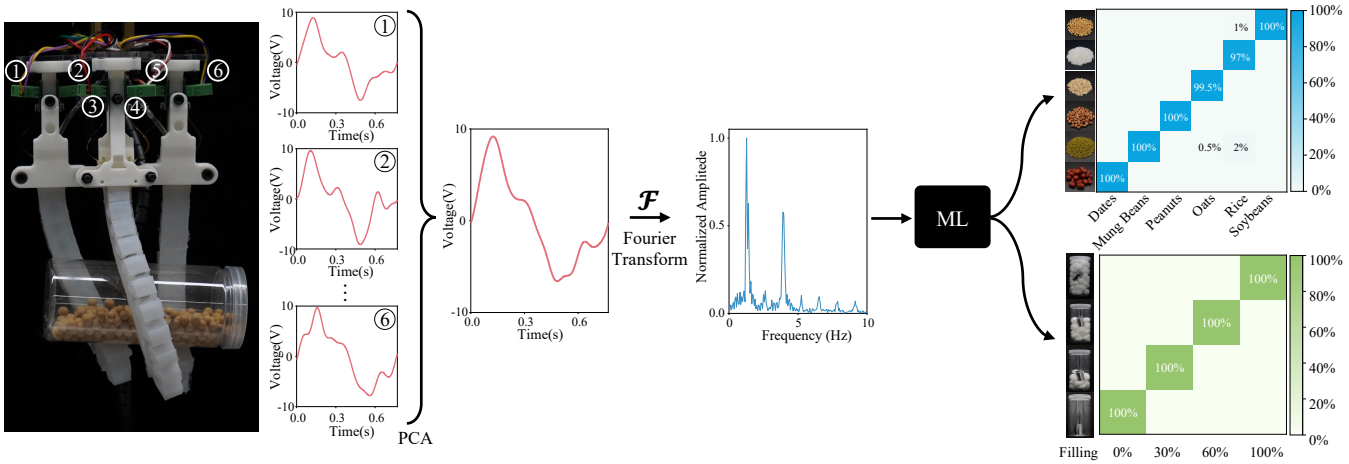


Fig. 7. Signal processing pipeline for grain identification and package quality inspection.

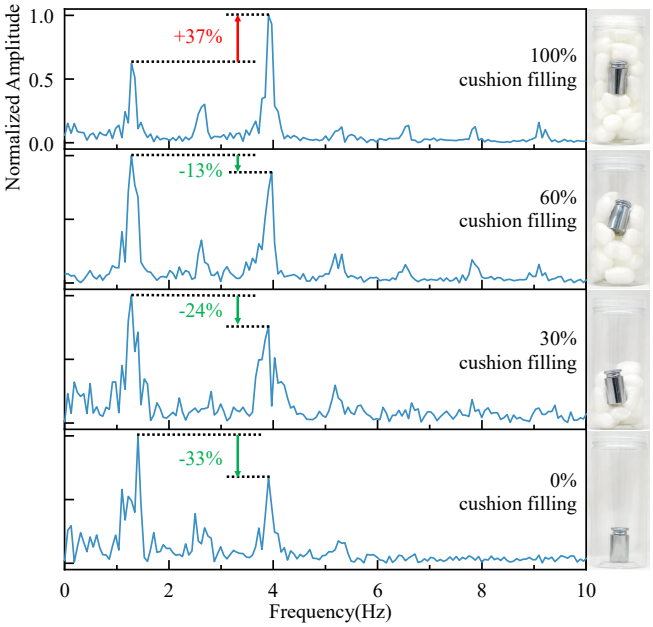


Fig. 8. The frequency profile of oscillating packages with different pellets filling levels.

to 0 to 10 Hz. Finally, the frequency domain samples are randomly divided into 400 training samples and 200 testing samples to train classification models. The data processing pipeline is shown in Fig. 7.

Here, we adopt classic machine learning methods to illustrate the expressing ability of the data in three settings: (i) 6 single ingredient grains, (ii) 9 dual-ingredients grains, and (iii) 15 combinations with single and double ingredients grains (Fig. 6). All the models are implemented by the classification learner toolbox of MATLAB. Due to the well-designed sensors and high data efficiency, without computationally expensive deep learning methods, the classic subspace k-nearest neighbors algorithm (KNN) [35], and kernel support vector machine (SVM) [36] can achieve excellent accuracy (Table I) in three granular object identification tasks.

TABLE I

PERFORMANCE COMPARISON IN CLASSIFICATION.

| ML Method | 6 grains | 9 mixtures | 15 together | Filling |
|---|---|---|---|---|
| KNN | 93.0% | 80.9% | 76.8% | 99.8% |
| Subspace KNN | 99.4% | 97.4% | **97.3%** | **100.0%** |
| Linear SVM | 98.2% | 84.9% | 81.3% | 86.8% |
| Kernel SVM | **99.9%** | **97.8%** | 96.2% | 99.4% |

### C. *Package quality inspection*

In the logistics industry, cushioning pellets are used to prevent the vibration and collision of fragile goods inside their package during transporting. Hence, we designed a package quality inspection experiment to demonstrate a potential industry application for soft robots' proprioceptive vibration sensing. The experiment uses the same soft gripper set-up with the grain classification task, while the grain is substituted into expandable polyethylene (EPE) pellet and a 100 g balance weight. The level of cushion pellet filling determines the packaging quality. During the oscillation motion, it is intuitive that the higher filling level will reduce the center of gravity shift. This situation can be directly observed by the frequency profile changes. As shown in Fig. 8, the normalized amplitude of the second spectrum peak gradually surpasses the first peak with four increased filling levels. The subspace KNN classification model also achieves perfect results in determining four filling conditions. (Refer to Table I).

## V. CONCLUSION AND DISCUSSION

This paper proposes a novel e-skin to enable soft robot proprioceptive vibration sensation. The e-skin is fabricated by the massively producible screen printing stretchable liquid metal circuit, and robots equipped with the e-skin can easily distinguish subtle vibration differences. Our experiments revealed that even traditional classifiers can accurately classify the vibration signal from shaking different granules and evaluate the packaging quality by their vibration responses.

Nevertheless, some features of our e-skin design have not been thoroughly investigated, such as independently leading-out signals from each sensory leaf of the e-skin to analyze multi-point vibration status. In the future, many applications of soft robots' closed-loop control, dexterous manipulation, and intelligent recognition tasks can leverage proprioceptive vibration sensation to realize. For example, suppress undesired vibration by neuroadaptive control, detect object slippage during manipulation, and discriminate liquid substances by shaking.

## ACKNOWLEDGEMENT

We address special thanks to Mr. Jin Shang from Jiang's Group at Southern University of Science and Technology for his guidance on screen printing of MPC circuit and Mr. Xiao Xiao from Wu's Group at National University of Singapore for his assistance on COMSOL simulation.

## REFERENCES

[1] J. C. Yang, J. Mun, S. Y. Kwon, S. Park, Z. Bao, and S. Park, "Electronic skin: Recent progress and future prospects for skin-attachable devices for health monitoring, robotics, and prosthetics," *Advanced Materials*, vol. 31, no. 48, p. e1904765, 2019.

[2] D. Rus and M. T. Tolley, "Design, fabrication and control of soft robots," *Nature*, vol. 521, no. 7553, pp. 467–75, 2015.

[3] H. Wang, M. Totaro, and L. Beccai, "Toward perceptive soft robots: Progress and challenges," *Advanced Science*, vol. 5, no. 9, p. 1800541, 2018.

[4] C. M. Boutry, M. Negre, M. Jorda, O. Vardoulis, A. Chortos, O. Khatib, and Z. Bao, "A hierarchically patterned, bioinspired e-skin able to detect the direction of applied pressure for robotics," *Science Robotics*, vol. 3, no. 24, p. eaau6914, 2018.

[5] Y. Li, Y. Chen, T. Ren, and Y. Hu, "Passive and active particle damping in soft robotic actuators," in *2018 IEEE International Conference on Robotics and Automation (ICRA)*, May. 2018, pp. 1547–1552.

[6] B. Shih, D. Shah, J. Li, T. G. Thuruthel, Y. L. Park, F. Iida, Z. Bao, R. Kramer-Bottiglio, and M. T. Tolley, "Electronic skins and machine learning for intelligent soft robots," *Science Robotics*, vol. 5, no. 41, p. eaaz9239, 2020.

[7] L. Tang, S. Cheng, L. Zhang, H. Mi, L. Mou, S. Yang, Z. Huang, X. Shi, and X. Jiang, "Printable metal-polymer conductors for highly stretchable bio-devices," *iScience*, vol. 4, pp. 302–311, 2018.

[8] S. Niu, Y. Liu, S. Wang, L. Lin, Y. S. Zhou, Y. Hu, and Z. L. Wang, "Theoretical investigation and structural optimization of single-electrode triboelectric nanogenerators," *Advanced Functional Materials*, vol. 24, no. 22, pp. 3332–3340, 2014.

[9] Y. Luo, Z. Wang, J. Wang, X. Xiao, Q. Li, W. Ding, and H. Y. Fu, "Triboelectric bending sensor based smart glove towards intuitive multi-dimensional human-machine interfaces," *Nano Energy*, vol. 89, p. 106330, 2021.

[10] B. Mosadegh, P. Polygerinos, C. Keplinger, S. Wennstedt, R. F. Shepherd, U. Gupta, J. Shim, K. Bertoldi, C. J. Walsh, and G. M. Whitesides, "Pneumatic networks for soft robotics that actuate rapidly," *Advanced Functional Materials*, vol. 24, no. 15, pp. 2163–2170, 2014.

[11] B. Shih, D. Drotman, C. Christianson, Z. Huo, R. White, H. I. Christensen, and M. T. Tolley, "Custom soft robotic gripper sensor skins for haptic object visualization," in *2017 IEEE/RSJ International Conference on Intelligent Robots and Systems (IROS)*, Sept. 2017, pp. 494–501.

[12] Y. Yan, Z. Hu, Z. Yang, W. Yuan, C. Song, J. Pan, and Y. Shen, "Soft magnetic skin for super-resolution tactile sensing with force self-decoupling," *Science Robotics*, vol. 6, no. 51, p. eabc8801, 2021.

[13] X. Qu, Z. Liu, P. Tan, C. Wang, Y. Liu, H. Feng, D. Luo, Z. Li, and Z. L. Wang, "Artificial tactile perception smart finger for material identification based on triboelectric sensing," *Science Advances*, vol. 8, no. 31, p. eabq2521, 2022.

[14] Z. Song, J. Yin, Z. Wang, C. Lu, Z. Yang, Z. Zhao, Z. Lin, J. Wang, C. Wu, J. Cheng, Y. Dai, Y. Zi, S.-L. Huang, X. Chen, J. Song, G. Li, and W. Ding, "A flexible triboelectric tactile sensor for simultaneous material and texture recognition," *Nano Energy*, vol. 93, p. 106798, 2021.

[15] E. W. Hawkes, C. Majidi, and M. T. Tolley, "Hard questions for soft robotics," *Science Robotics*, vol. 6, no. 53, p. eabg6049, 2021.

[16] R. Franke, J. Malzahn, T. Nierobisch, F. Hoffmann, and T. Bertram, "Vibration control of a multi-link flexible robot arm with fiber-bragg-grating sensors," in *2009 IEEE International Conference on Robotics and Automation (ICRA)*, May. 2009, pp. 3365–3370.

[17] H. Zhao, K. O'Brien, S. Li, and R. F. Shepherd, "Optoelectronically innervated soft prosthetic hand via stretchable optical waveguides," *Science Robotics*, vol. 1, no. 1, p. eaai7529, 2016.

[18] H. Bai, S. Li, J. Barreiros, Y. Tu, C. R. Pollock, and R. F. Shepherd, "Stretchable distributed fiber-optic sensors," *Science*, vol. 370, no. 6518, pp. 848–852, 2020.

[19] R. L. Truby, C. D. Santina, and D. Rus, "Distributed proprioception of 3D configuration in soft, sensorized robots via deep learning," *IEEE Robotics and Automation Letters*, vol. 5, no. 2, pp. 3299–3306, 2020.

[20] T. G. Thuruthel, B. Shih, C. Laschi, and M. T. Tolley, "Soft robot perception using embedded soft sensors and recurrent neural networks," *Science Robotics*, vol. 4, no. 26, p. eaav1488, 2019.

[21] S. S. Baishya and B. Bäuml, "Robust material classification with a tactile skin using deep learning," in *2016 IEEE/RSJ International Conference on Intelligent Robots and Systems (IROS)*, Oct. 2016, pp. 8–15.

[22] H.-J. Huang, X. Guo, and W. Yuan, "Understanding dynamic tactile sensing for liquid property estimation," in *2022 Robotics: Science and Systems (RSS)*, Jul. 2022.

[23] C. L. Chen, J. O. Snyder, and P. J. Ramadge, "Learning to identify container contents through tactile vibration signatures," in *2016 IEEE International Conference on Simulation, Modeling, and Programming for Autonomous Robots (SIMPAR)*, Dec. 2016, pp. 43–48.

[24] R. Hinchet, H. J. Yoon, H. Ryu, M. K. Kim, E. K. Choi, D. S. Kim, and S. W. Kim, "Transcutaneous ultrasound energy harvesting using capacitive triboelectric technology," *Science*, vol. 365, no. 6452, p. 491, 2019.

[25] H. Zhao, M. Shu, Z. Ai, Z. Lou, K. W. Sou, C. Lu, Y. Jin, Z. Wang, J. Wang, C. Wu, Y. Cao, X. Xu, and W. Ding, "A highly sensitive triboelectric vibration sensor for machinery condition monitoring," *Advanced Energy Materials*, p. 2201132, 2022.

[26] F.-R. Fan, Z.-Q. Tian, and Z. L. Wang, "Flexible triboelectric generator," *Nano energy*, vol. 1, no. 2, pp. 328–334, 2012.

[27] Y. Luo, X. Xiao, J. Chen, Q. Li, and H. Fu, "Machine-learning-assisted recognition on bioinspired soft sensor arrays," *ACS nano*, vol. 16, no. 4, pp. 6734–6743, 2022.

[28] C. Wu, A. C. Wang, W. Ding, H. Guo, and Z. L. Wang, "Triboelectric nanogenerator: a foundation of the energy for the new era," *Advanced Energy Materials*, vol. 9, no. 1, p. 1802906, 2019.

[29] S. Liu, Y. Li, W. Guo, X. Huang, L. Xu, Y.-C. Lai, C. Zhang, and H. Wu, "Triboelectric nanogenerators enabled sensing and actuation for robotics," *Nano Energy*, vol. 65, p. 104005, 2019.

[30] J. Lu, Z. Miao, Z. Wang, Y. Liu, D. Zhu, J. Yin, F. Tang, X. Wang, W. Ding, and M. Zhang, "Piezoelectric soft robot driven by mechanical energy," *Nano Research*, pp. 1–10, 2022.

[31] H. Zou, Y. Zhang, L. Guo, P. Wang, X. He, G. Dai, H. Zheng, C. Chen, A. C. Wang, C. Xu *et al.*, "Quantifying the triboelectric series," *Nature Communications*, vol. 10, no. 1, pp. 1–9, 2019.

[32] L. Marechal, P. Balland, L. Lindenroth, F. Petrou, C. Kontovounisios, and F. Bello, "Toward a common framework and database of materials for soft robotics," *Soft Robotics*, vol. 8, no. 3, pp. 284–297, 2021.

[33] D. Zrnic and D. Swatik, "On the resistivity and surface tension of the eutectic alloy of gallium and indium," *Journal of the Less Common Metals*, vol. 18, no. 1, pp. 67–68, 1969.

[34] H. Yu, X. He, W. Ding, Y. Hu, D. Yang, S. Lu, C. Wu, H. Zou, R. Liu, C. Lu *et al.*, "A self-powered dynamic displacement monitoring system based on triboelectric accelerometer," *Advanced Energy Materials*, vol. 7, no. 19, p. 1700565, 2017.

[35] T. K. Ho, "Nearest neighbors in random subspaces," in *Joint IAPR international workshops on statistical techniques in pattern recognition (SPR) and structural and syntactic pattern recognition (SSPR)*. Springer, 1998, pp. 640–648.

[36] C. Cortes and V. Vapnik, "Support-vector networks," *Machine Learning*, vol. 20, no. 3, pp. 273–297, 1995.